

San Andreas Fault tremor and retrograde metamorphism

Åke Fagereng¹ and Johann F. A. Diener¹

Received 10 September 2011; revised 28 October 2011; accepted 1 November 2011; published 8 December 2011.

[1] Tectonic tremor is an enigmatic low-frequency seismic phenomenon mainly observed in subduction zones, but also documented along the deep extension of the central San Andreas Fault. The physical mechanisms behind this unusual seismic event are not yet determined for any tectonic setting; however, low effective stress conditions arising from metamorphic fluid production are commonly inferred for subduction-related tremor. We investigate the petrologic conditions at which the San Andreas tectonic tremor is inferred to occur through calculations of the pressure–temperature–time evolution of stable mineral assemblages and their water content in the dominant lithologies of the Franciscan Complex. We find that tremor locations around Parkfield and Cholame are currently experiencing retrograde metamorphic conditions. Within the temperature–depth conditions of observed tremor activity, at approximately 500°C and 20 km depth, several mineralogical transitions may occur in cooling greywacke and mafic rocks, leading to localised, significant removal of free water and an associated volume decrease. This indicates that, contrary to subduction-related tremor, tremor on the San Andreas Fault is not linked to prograde, crustal metamorphic fluid production within the fault zone; rather it might be related to mantle-derived fluids from below the tremor zone, and/or fault zone weakening that occurs as phyllosilicates replace more competent and granular mineral phases. **Citation:** Fagereng, Å., and J. F. A. Diener (2011), San Andreas Fault tremor and retrograde metamorphism, *Geophys. Res. Lett.*, 38, L23303, doi:10.1029/2011GL049550.

1. Introduction

[2] Tectonic tremor – a recently discovered low-frequency seismic phenomenon – has been observed on the deep extension of the central San Andreas Fault (SAF) in the region surrounding Parkfield and Cholame (Figure 1a) [Nadeau and Dolenc, 2005; Nadeau and Guilhem, 2009; Shelly, 2010; Shelly and Hardebeck, 2010]. Globally, such tremor signals have been observed predominantly along subduction thrust interfaces [e.g., Rubinstein et al., 2010; Beroza and Ide, 2011]. Low effective stress and high pore fluid pressures are suspected to be required for tremor activity, based on modelling studies [e.g., Liu and Rice, 2007] and correlations between tremor locations and zones of high V_p/V_s , low V_p , high seismic reflectivity, and inferred locations of metamorphic dehydration reactions [e.g., Obara, 2002; Shelly et al., 2006; Peacock, 2009; Rubinstein et al., 2010; Beroza and Ide, 2011; Fagereng and Diener, 2011].

[3] As for subduction-related tremor, a low effective stress is implied in the tremor source of the SAF because tremor activity is modulated by teleseismic waves and earth tides [Peng et al., 2009; Thomas et al., 2009]. However, as the SAF is not associated with actively subducting oceanic crust, it does not have the ready source of metamorphic fluids found in subduction margins. Thus, the SAF either has an alternative fluid source along its deep extension [Nadeau and Dolenc, 2005], or tremor on the SAF is not associated with high fluid pressure. Possible alternative fluid sources include: (1) metamorphic dehydration of the crustal Franciscan Complex [Irwin and Barnes, 1975]; (2) fluids migrating upwards from the viscous lower crust and upper mantle at superhydrostatic pressures [Rice, 1992; Kennedy et al., 1997]; and (3) an upward fluid flux from a mantle wedge that was serpentinized during subduction before the formation of the SAF, and would dehydrate after a transition to strike-slip tectonics [Kirby et al., 2002; Fulton and Saffer, 2009]. That some overpressured fluids are locally present around the deep San Andreas is inferred from seismic evidence, including a low-velocity zone at the base of the Franciscan Complex [Trehu and Wheeler, 1987], and high V_p/V_s in the lower crust interpreted as overpressured water in serpentinite or fluid-saturated schist [Ozacar and Zandt, 2009].

[4] Besides the difference in tectonic setting and fluid availability, Nadeau and Dolenc [2005] found that SAF tremor is less frequent, lasts for shorter duration and releases less energy than subduction-related tremor. There are, however, also similarities between SAF and subduction thrust tremor as both are localised along a plate boundary scale fault zone below the depth of the seismogenic zone, and have waveforms consisting of repeated events with a dominant frequency content of 2–8 Hz [Nadeau and Dolenc, 2005; Shelly, 2010; Shelly and Hardebeck, 2010]. Importantly, the tremor activity on the SAF is also strongly aligned along the down-dip continuation of the fault, indicating that the fault zone extends as a localised feature to the base of the crust, and that the tremor occurs within the deep fault zone [Shelly et al., 2009; Shelly and Hardebeck, 2010].

[5] Here we investigate the occurrence of SAF tremor by constraining the likely petrologic conditions and metamorphic evolution of rocks in the tremor source region for the Parkfield – Cholame area. We combine thermal models presented by Sass et al. [1997] and Guzowski and Furlong [2002] with modern quantitative mineral equilibria modelling [Powell and Holland, 1988] to determine the pressure–temperature–time ($P - T - t$) evolution of the deep SAF, and assess possible fluid sources and sinks related to metamorphic processes in the SAF tremor source region. The SAF at Parkfield separates Salinian granite to the SW and the Franciscan Complex overlain by Great Valley sedimentary rocks to the NE. However, as the fault zone at tremor depths seems to localise primarily within rocks of the Franciscan Complex [Eberhart-Phillips and Michael, 1993; Ozacar and

¹Department of Geological Sciences, University of Cape Town, Rondebosch, South Africa.

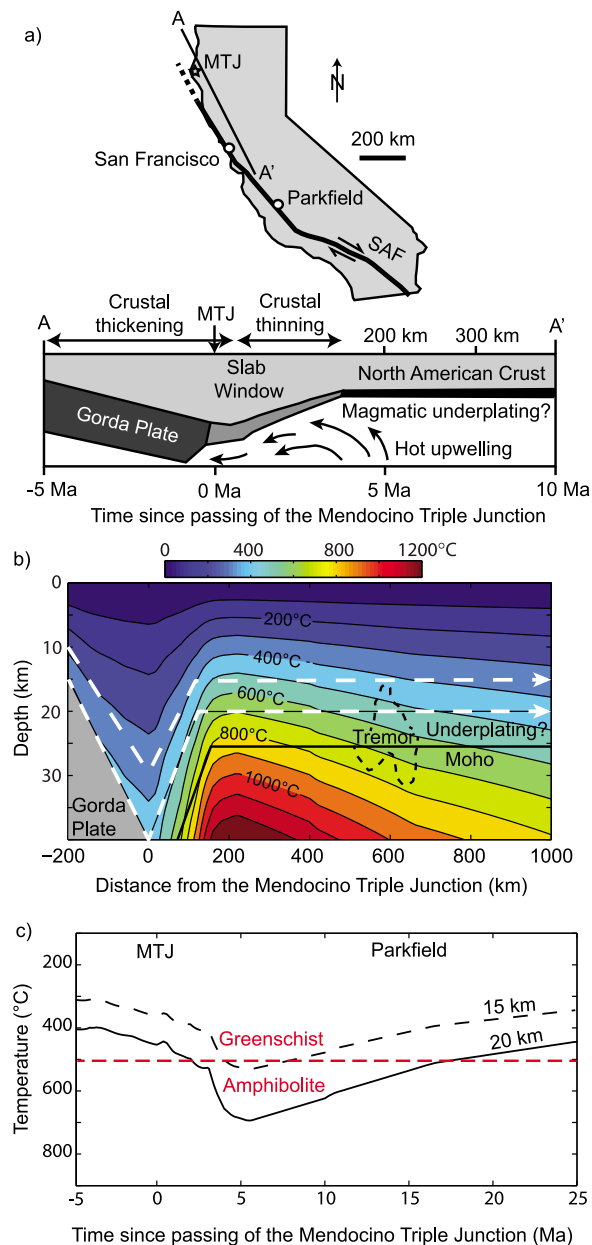


Figure 1. Locations, evolution and thermal structure of the San Andreas Fault. (a) Map of California showing locations of the San Andreas Fault and Parkfield, and a schematic cross section of the crust of the North American Plate [after *Guzofski and Furlong, 2002*]. (b) Calculated temperature contours (100°C intervals) in a vertical section along the San Andreas Fault. White arrows show approximate particle paths for rocks presently at 15 and 20 km depth below Parkfield. Approximate tremor source region after *Shelly and Hardebeck [2010]*, Moho depth at Parkfield after *Ozacar and Zandt [2009]*. (c) Temperature against time since the passing of the Mendocino Triple Junction, for selected depths on the vertical San Andreas Fault. The greenschist-amphibolite facies boundary as calculated in Figure 2 is shown by a dashed red line.

Zandt, 2009], we investigate the metamorphic evolution of greywacke and hydrated basalt, the dominant lithologies of the Franciscan mélangé [*Wakabayashi, 1999*].

2. Methods

2.1. Thermal Structure

[6] *Guzofski and Furlong [2002]* suggested that the thermal evolution of rocks along the SAF is controlled by the northward migration of the Mendocino Triple Junction (MTJ) (Figure 1a). North of the MTJ the Gorda subplate is subducting towards the east underneath the North American plate, cooling the overlying lithosphere, whereas south of the MTJ upwelling of asthenospheric mantle into a ‘slab window’ causes significant heating, consistent with surface heat flow measurements [*Lachenbruch and Sass, 1980; Sass et al., 1997; Guzofski and Furlong, 2002*]. Within this model, uniformly distributed crustal thickening occurs north of the MTJ, whereas the slab window is associated with uniform crustal thinning (Figure 1a) [*Furlong and Govers, 1999*].

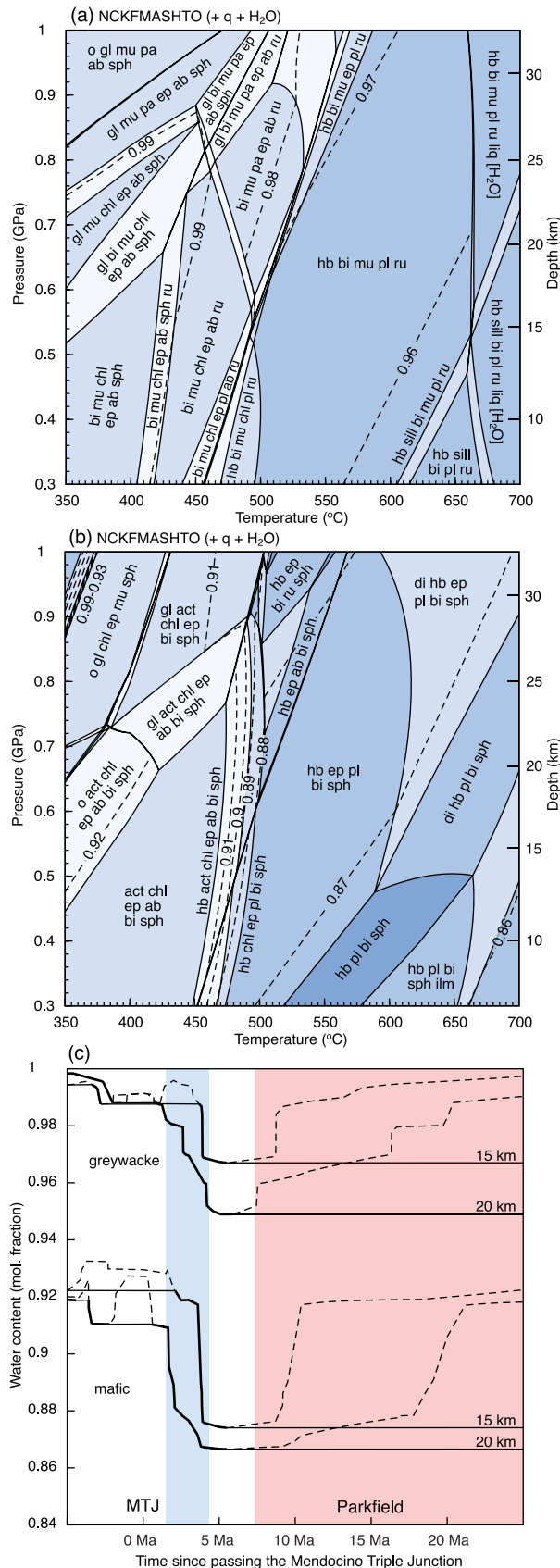
[7] We estimate a thermal structure parallel to the SAF (Figure 1b), by solving the steady-state 1-D conductive heat equation:

$$dT/dz = \left[(q_s - DA_0)z + D^2A_0(1 - e^{-z/D}) \right] / K \quad (1)$$

for a column of crust as it evolves after passage of the MTJ. We fix surface heat flow (q_s) at values determined theoretically by *Guzofski and Furlong [2002]* and heat flow data presented by *Sass et al. [1997]*, assume a constant thermal conductivity (K) of $2.5 \text{ W m}^{-1} \text{ K}^{-1}$, and take surface radiogenic heat production (A_0) as $1.5 \mu\text{W m}^{-3}$, decaying exponentially over 15 km depth (D). Because movement on the SAF is dominantly horizontal, we ignore effects of erosion. This model is not new, but essentially produces a 2-D thermal field in space (Figure 1b), based on the 1-D geotherms calculated by *Sass et al. [1997]*, updated to fit the thermal model of *Guzofski and Furlong [2002]* for locations within ± 200 km of the MTJ. By substituting time for distance to the MTJ, assuming the MTJ migrates northward at a rate of 40 km Ma^{-1} [*Atwater and Stock, 1998*], this model produces a 2-D thermal field in time (Figure 1c) [*Guzofski and Furlong, 2002*]. As the MTJ is inferred to have collided with the North American continent 25–29 Ma [*Atwater and Stock, 1998*], we suggest this time conversion is applicable for at least 1000 km along the San Andreas Fault, assuming slip rate has not changed significantly since the formation of the SAF.

2.2. Mineral Equilibria Modelling

[8] Mineral equilibria calculations utilised the program THERMOCALC (version 3.33; released 26/10/2009) with the updated internally-consistent thermodynamic dataset of *Holland and Powell [1998]* (version 5) and the following activity-composition models: glaucophane, actinolite and hornblende [*Diener et al., 2007*]; omphacite and diopside [*Green et al., 2007*]; biotite, garnet and silicate melt [*White et al., 2007*]; muscovite and paragonite [*Coggon and Holland, 2002*]; and epidote, lawsonite, sillimanite, chlorite, rutile, titanite, albite, quartz and water [*Holland and Powell, 1998*]. Calculations were performed in the $\text{Na}_2\text{O-CaO-K}_2\text{O-FeO-MgO-Al}_2\text{O}_3\text{-SiO}_2\text{-H}_2\text{O-TiO}_2\text{-O}$ (NCKFMASHTO) chemical system for an average Franciscan greywacke



composition [Bloxam, 1956; Ernst, 1971], and a typical mid-ocean ridge basalt [Sun and McDonough, 1989]. The calculated phase diagrams (Figures 2a and 2b) show the stable mineral assemblages in each of these rocks as a function of P and T . The water content of the rocks is shown as contours representing the maximum amount of crystal-bound water as a fraction of an arbitrary maximum value, chosen such that the mineral assemblages are water saturated for all P - T conditions. Closely-spaced contours correspond to dehydration reactions and denote conditions of water release with increasing T , or potential water consumption with decreasing T .

3. Results

[9] The estimated thermal profile (Figure 1b) shows low temperatures and geothermal gradients to the north of the MTJ, corresponding to the position of the subducting Gorda Plate (Figures 1a and 1b), and probably reflecting crustal thickening [Furlong and Govers, 1999]. South of the MTJ the profile shows high temperatures and condensed isotherms that correspond to the current slab window. South of the current slab window, temperatures and geothermal gradients gradually decrease because of magmatic underplating and increasing distance from the upwelling centre near the MTJ [cf. Guzowski and Furlong, 2002].

[10] The estimated P - T - t paths indicate significant heating after passage of the edge of the Gorda slab, followed by slow cooling after passage of the upwelling centre south of the MTJ (Figure 1c) [Guzowski and Furlong, 2002]. At Parkfield, ~600 km away from the MTJ (Figure 1a), temperature at the base of the seismogenic zone (~15 km) is estimated at 410°C (Figure 1b), within the commonly inferred range of 350–450°C for quartzofeldspathic crust [Sibson, 1984], whereas for the range of tremor depths, 16–28 km (Figure 1b) [Shelly and Hardebeck, 2010], our temperature estimates are 450 to 770°C (Figure 1b).

[11] The P - T pseudosections for both greywacke and basalt (Figures 2a and 2b) show that, at the start of the

Figure 2. Mineral assemblage and fluid evolution of the deep San Andreas Fault. P - T pseudosections calculated for (a) greywacke and (b) mafic rocks from the Franciscan complex, showing stable mineral assemblages and amounts of crystal-bound water. Mineral abbreviations are: ab, albite; act, actinolite; bi, biotite; chl, chlorite; di, diopside; ep, epidote; gl, glaucophane; hb, hornblende (*sensu lato*); ilm, ilmenite; liq, silicate melt; mu, muscovite; o, omphacite; pa, paragonite; pl, plagioclase; ru, rutile; sill, sillimanite; sph, titanite. In addition to the indicated minerals, all fields also contain quartz (q) and water (H₂O), except where indicated by [H₂O]. (c) Fluid content evolution of greywacke and mafic rocks currently at 15 and 20 km depth below Parkfield along the P - T - t paths in Figure 1c. Thick solid lines denote periods of fluid production and fluid presence whereas thin solid lines denote periods of fluid absence and potential fluid uptake during retrograde metamorphism if fluid is available. Dashed lines are the calculated fluid saturation curves for fluid-absent rocks. Voluminous fluid release occurs between 2–4 Ma after passing of the MTJ (blue shading) and rocks become progressively more fluid-undersaturated and capable of retrograde reactions from 7 Ma after passing of the MTJ (red shading).

tremor zone at 16–20 km depth and 450–520°C, these rocks may undergo a series of mineralogical transitions corresponding to the conversion from greenschist to amphibolite facies mineral assemblages. With cooling, the stable assemblage in greywacke can potentially change from quartz-plagioclase-hornblende-biotite-muscovite above 520°C to quartz-albite-muscovite-epidote-biotite-chlorite below 480°C (Figure 2a). Similarly, the assemblage in basalt can change from hornblende-quartz-epidote-plagioclase-biotite above 510°C to epidote-actinolite-chlorite-albite-quartz-biotite below 480°C (Figure 2b). However, these changes require the addition of water (2.2 mol % for greywacke and 3.5 mol % for basalt; Figure 2c) to these rocks for the reactions to go to completion. Therefore, at $T \sim 500^\circ\text{C}$ and in the presence of an aqueous fluid, hornblende and plagioclase are replaced by chlorite, epidote and albite in greywacke compositions, and hornblende and plagioclase are replaced by actinolite, chlorite and albite in basaltic rocks. These mineralogical changes would result in a $\sim 3\%$ decrease in the solid phase molar volume of both rock types.

[12] Other mineralogical changes that occur in the $P - T$ range of observed tremor is the introduction of silicate melt at $\sim 660^\circ\text{C}$ in greywacke and the introduction of diopside at $\sim 600^\circ\text{C}$ in basalt (Figure 2). However, these changes are not as dramatic as the reactions occurring at 500°C , and cause less significant changes to potential fluid content (Figure 2c).

[13] Importantly for our study, the MTJ passed Parkfield at approximately 15 Ma (Figure 1c). The geothermal gradient at Parkfield therefore reached a maximum with the passage of the slab window about 10 Ma, and has been cooling since. As fluid production through dehydration reactions generally only occurs with increasing temperature (Figure 2), it can be argued that there has been no fluid produced in the crust around the central SAF in the last 10 Ma (Figure 2c). Our calculations therefore support the conclusion of *Fulton et al.* [2009] that crustal dehydration does not supply significant fluids to the SAF after ~ 6 Ma following the passing of the MTJ. Thus, the only metamorphic processes potentially occurring in the tremor source at the deep extension of the central SAF are rehydration reactions defining the amphibolite to greenschist facies transition. These retrograde reactions would involve the consumption of available free water and lead to changes in mineralogy - notably the introduction of significant amounts of chlorite.

4. Discussion and Conclusions

4.1. Conditions in the SAF Tremor Source Region

[14] The central SAF is inferred to be cooling (Figure 1c) and potentially undergoing water-consuming, retrograde metamorphism, in sharp contrast to the localised water release expected in zones of subduction-related tremor activity [*Fagereng and Diener*, 2011]. The northern SAF, just south of the MTJ, on the other hand, is heating up (Figure 1b) and one might speculate whether dehydration reactions occurring within 100 km of the MTJ (Figure 2c) could be responsible for as yet undetected tremor activity.

[15] Rocks within the tremor source region at Parkfield have cooled to temperatures at or below the amphibolite to greenschist transition (Figure 1c). Importantly, unless enough water for complete retrogression to greenschist facies assemblages has been previously supplied, the rocks will remain

fluid-undersaturated and continue to consume available free water. Crustal rocks at the deep extension of the SAF cannot release water under these cooling conditions (Figure 2c), and an alternative fluid source is required for metamorphic reactions and/or elevated fluid pressures to occur. Observations of low V_p , high V_p/V_s , and areas of high seismic reflectivity within and around the deep SAF indicate that, at least locally, significant fluid pressures occur within the crust surrounding the SAF. The most plausible source of this fluid is the underlying mantle [*Rice*, 1992; *Kennedy et al.*, 1997], specifically from dehydration of serpentinized mantle at depth northeast of the SAF [*Kirby et al.*, 2002; *Fulton and Saffer*, 2009].

[16] That fault zone rheology is significantly affected by retrograde metamorphic reactions has long been recognized [e.g., *Wintsch et al.*, 1995; *Imber et al.*, 1997], and similarly it is generally accepted that fault zones provide high permeability fluid pathways that allow them to preferentially undergo retrogression, relative to surrounding, intact crust [e.g., *Corbett and Phillips*, 1981; *Kerrich et al.*, 1984]. Therefore, the observation that tremor localizes to the deep extension of the SAF indicates that the tremor localizes to a zone of preferential fluid flow and retrograde metamorphism, where deformation is preferentially concentrated because of fluid-reaction weakening [e.g., *Wintsch et al.*, 1995].

4.2. Implications for Tremorogenic Conditions

[17] If tectonic tremor on the SAF is related to ongoing metamorphic retrogression, requiring an inflow of free water, it appears that the tremor-generating conditions here differ from those during tremor in dehydrating, heating subducting slabs. There are two obvious effects from the retrograde reactions that potentially occur as Franciscan Complex-derived fault rocks cool below 500°C : (1) a small negative volume change, and (2) changes to the mineralogy. It is possible that volume change alone may be capable of generating tremor-like seismic signals [*Burlini et al.*, 2009], but this does not explain evidence for tremor representing shear slip within the fault zone [e.g., *Thomas et al.*, 2009; *Nadeau and Guilhem*, 2009]. On the other hand, the mineralogical transition may lead to the creation of an interconnected network of chlorite - causing significant fault zone weakening [cf. *Imber et al.*, 1997], particularly under wet conditions [*Moore and Lockner*, 2004]. Such a network is also likely to be relatively impermeable, potentially channelling fluids from below the seismogenic fault along a narrow, impermeable fault zone. Thus, if fluids can be derived from outside the cooling, fluid-consuming, tremor source region, low effective stress and fluid-reaction weakening may co-exist within a zone of retrograde metamorphic conditions.

[18] In conclusion, we have shown that retrograde metamorphic reactions may occur in greywacke and basalt within Franciscan mélange rock assemblages cooling below $\sim 500^\circ\text{C}$ if free water is available. Therefore retrograde reactions may occur in the $P - T$ range where tremor is observed on the deep extension of the SAF. It is not clear whether retrogression is directly related to or responsible for tremor, but the potential mineralogical changes are associated with likely significant fault zone weakening and change in frictional properties. The amount of retrogression is highly dependent on available free fluid, therefore potentially leading to a heterogeneous distribution of tremor on this fault. Given that the metamorphic path and fluid conditions

predicted here for SAF tremor are very different to those inferred for subduction thrust tremor [Shelly *et al.*, 2006; Peacock, 2009; Fagereng and Diener, 2011], it appears that tremor can occur under a variety of metamorphic and fluid regimes and does not require one specific set of these criteria. This suggests that the actual tremorogenic conditions may be more fundamental, such as localised changes in fluid pressure or frictional properties, and not dependent on specific *P-T* trajectories or conditions.

[19] **Acknowledgments.** Å.F. and J.F.A.D. acknowledge financial support from separate Research Development grants from the University of Cape Town. Constructive comments from D. Saffer and an anonymous reviewer significantly improved the paper and are sincerely appreciated. M. Wyssession is thanked for editorial handling.

[20] The Editor thanks Demian Saffer and an anonymous reviewer for their assistance in evaluating this paper.

References

- Atwater, T., and J. M. Stock (1998), Pacific-North America plate tectonics of the Neogene southwestern United States: An update, *Int. Geol. Rev.*, **40**, 375–402, doi:10.1080/00206819809465216.
- Beroza, G. C., and S. Ide (2011), Slow earthquakes and nonvolcanic tremor, *Annu. Rev. Earth Planet. Sci.*, **39**, 271–296, doi:10.1146/annurev-earth-040809-152531.
- Bloxam, T. W. (1956), Jadeite-bearing metagraywackes in California, *Am. Mineral.*, **41**, 488–496.
- Burlini, L., G. Di Toro, and P. Meredith (2009), Seismic tremor in subduction zones: Rock physics evidence, *Geophys. Res. Lett.*, **36**, L08305, doi:10.1029/2009GL037735.
- Coggon, R., and T. J. B. Holland (2002), Mixing properties of phengitic micas and revised garnet-phengite thermobarometers, *J. Metamorph. Geol.*, **20**, 683–696, doi:10.1046/j.1525-1314.2002.00395.x.
- Corbett, G. J., and G. N. Phillips (1981), Regional retrograde metamorphism of a high-grade terrain: The Willyama Complex, Broken Hill, Australia, *Lithos*, **14**, 59–73, doi:10.1016/0024-4937(81)90037-2.
- Diener, J. F. A., R. Powell, R. W. White, and T. J. B. Holland (2007), A new thermodynamic model for clino- and orthoamphiboles in the system Na₂O-CaO-FeO-MgO-Al₂O₃-SiO₂-H₂O, *J. Metamorph. Geol.*, **25**, 631–656, doi:10.1111/j.1525-1314.2007.00720.x.
- Eberhart-Phillips, D., and A. J. Michael (1993), Three-dimensional velocity structure, seismicity, and fault structure in the Parkfield Region, central California, *J. Geophys. Res.*, **98**, 15,737–15,758, doi:10.1029/93JB01029.
- Ernst, W. G. (1971), Petrologic reconnaissance of Franciscan metagraywackes from the Diablo Range, central California Coast Ranges, *J. Petrol.*, **12**, 413–437.
- Fagereng, Å., and J. F. A. Diener (2011), Non-volcanic tremor and discontinuous slab dehydration, *Geophys. Res. Lett.*, **38**, L15302, doi:10.1029/2011GL048214.
- Fulton, P. M., and D. M. Saffer (2009), Potential role of mantle-derived fluids in weakening the San Andreas Fault, *J. Geophys. Res.*, **114**, B07408, doi:10.1029/2008JB006087.
- Fulton, P. M., D. M. Saffer, and B. A. Bekins (2009), A critical evaluation of crustal dehydration as the cause of an overpressured and weak San Andreas Fault, *Earth Planet. Sci. Lett.*, **284**, 447–454, doi:10.1016/j.epsl.2009.05.009.
- Furlong, K. P., and R. Govers (1999), Ephemeral crustal thickening at a triple junction: The Mendocino crustal conveyor, *Geology*, **27**, 127–130, doi:10.1130/0091-7613(1999)027<0127:ECTAAT>2.3.CO;2.
- Green, E. C. R., T. J. B. Holland, and R. Powell (2007), An order-disorder model for omphacitic pyroxenes in the system jadeite-diopside-hedenbergite-acmite, with applications to eclogitic rocks, *Am. Mineral.*, **92**, 1181–1189, doi:10.2138/am.2007.2401.
- Guzofski, C. A., and K. P. Furlong (2002), Migration of the Mendocino triple junction and ephemeral crustal deformation: Implications for California Coast Range heat flow, *Geophys. Res. Lett.*, **29**(1), 1012, doi:10.1029/2001GL013614.
- Holland, T. J. B., and R. Powell (1998), An internally consistent thermodynamic dataset for phases of petrological interest, *J. Metamorph. Geol.*, **16**, 309–343, doi:10.1111/j.1525-1314.1998.00140.x.
- Imber, J., R. E. Holdsworth, C. A. Butler, and G. A. Lloyd (1997), Fault-zone weakening processes along the reactivated Outer Hebrides Fault Zone, Scotland, *J. Geol. Soc.*, **154**, 105–109, doi:10.1144/gsjgs.154.1.0105.
- Irwin, W. P., and I. Barnes (1975), Effect of geologic structure and metamorphic fluids on seismic behaviour of the San Andreas Fault system in central and northern California, *Geology*, **3**, 713–716, doi:10.1130/0091-7613(1975)3<713:EOGSAM>2.0.CO;2.
- Kennedy, B. M., et al. (1997), Mantle liquids in the San Andreas Fault System, California, *Science*, **278**, 1278–1281, doi:10.1126/science.278.5341.1278.
- Kerrick, R., T. E. La Tour, and L. Willmore (1984), Fluid participation in deep fault zones: Evidence from geological, geochemical, and ¹⁸O/¹⁶O relations, *J. Geophys. Res.*, **89**, 4331–4343, doi:10.1029/JB089iB06p04331.
- Kirby, S., K. Wang and T. Brocher (2002), A possible deep, long-term source for water in the northern San Andreas Fault system: A ghost of Cascadia subduction past?, *Eos Trans. AGU*, **83**, Fall Meet. Suppl., Abstract S22B-1038.
- Lachenbruch, A. H., and J. H. Sass (1980), Heat flow and energetics of the San Andreas Fault Zone, *J. Geophys. Res.*, **85**, 6185–6222, doi:10.1029/JB085iB11p06185.
- Liu, Y., and J. R. Rice (2007), Spontaneous and triggered aseismic deformation transients in a subduction fault model, *J. Geophys. Res.*, **112**, B09404, doi:10.1029/2007JB004930.
- Moore, D. E., and D. A. Lockner (2004), Crystallographic controls on the frictional behavior of dry and water-saturated sheet structure minerals, *J. Geophys. Res.*, **109**, B03401, doi:10.1029/2003JB002582.
- Nadeau, R. M., and D. Dolenc (2005), Nonvolcanic tremors deep beneath the San Andreas Fault, *Science*, **307**, 389, doi:10.1126/science.1107142.
- Nadeau, R. M., and A. Guilhem (2009), Nonvolcanic tremor evolution and the San Simeon and Parkfield, California, earthquakes, *Science*, **325**, 191–193, doi:10.1126/science.1174155.
- Obara, K. (2002), Non-volcanic deep tremor associated with subduction in southwest Japan, *Science*, **296**, 1679–1681, doi:10.1126/science.1070378.
- Ozacar, A. A., and G. Zandt (2009), Crustal structure and seismic anisotropy near the San Andreas Fault at Parkfield, California, *Geophys. J. Int.*, **178**, 1098–1104, doi:10.1111/j.1365-246X.2009.04198.x.
- Peacock, S. M. (2009), Thermal and metamorphic environment of subduction zone episodic tremor and slip, *J. Geophys. Res.*, **114**, B00A07, doi:10.1029/2008JB005978.
- Peng, Z., J. E. Vidale, A. Wech, R. M. Nadeau, and K. M. Creager (2009), Remote triggering of tremor around the Parkfield section of the San Andreas Fault, *J. Geophys. Res.*, **114**, B00A06, doi:10.1029/2008JB006049.
- Powell, R., and T. J. B. Holland (1988), An internally consistent thermodynamic dataset with uncertainties and correlations: 3. Application, methods, worked examples and a computer program, *J. Metamorph. Geol.*, **6**, 173–204, doi:10.1111/j.1525-1314.1988.tb00415.x.
- Rice, J. R. (1992), Fault stress states, pore pressure distributions, and the weakness of the San Andreas fault, in *Fault Mechanics and Transport Properties of Rocks*, edited by B. Evans and T. Wong, pp. 475–503, Academic, San Diego, Calif., doi:10.1016/S0074-6142(08)62835-1.
- Rubinstein, J. L., D. R. Shelly, and W. L. Ellsworth (2010), Non-volcanic tremor: A window into the roots of fault zones, in *New Frontiers in Integrated Solid Earth Sciences*, edited by S. Cloetingh and J. Negendank, pp. 287–314, Springer, Dordrecht, Netherlands, doi:10.1007/978-90-481-2737-5_8.
- Sass, J. H., C. F. Williams, A. H. Lachenbruch, S. P. Galanis Jr., and F. V. Grubb (1997), Thermal regime of the San Andreas Fault near Parkfield, California, *J. Geophys. Res.*, **102**, 27,575–27,585, doi:10.1029/JB102iB12p27575.
- Shelly, D. R. (2010), Migrating tremors illuminate complex deformation beneath the seismogenic San Andreas Fault, *Nature*, **463**, 648–652, doi:10.1038/nature08755.
- Shelly, D. R., and J. L. Hardebeck (2010), Precise tremor source locations and amplitude variations along the lower-crustal central San Andreas Fault, *Geophys. Res. Lett.*, **37**, L14301, doi:10.1029/2010GL043672.
- Shelly, D. R., G. C. Beroza, S. Ide, and S. Nakamura (2006), Low-frequency earthquakes in Shikoku, Japan, and their relationship to episodic tremor and slip, *Nature*, **442**, 188–191, doi:10.1038/nature04931.
- Shelly, D. R., W. L. Ellsworth, T. Ryberg, C. Haberland, G. S. Fuis, J. Murphy, R. M. Nadeau, and R. Bürgmann (2009), Precise location of San Andreas Fault tremors near Cholame, California using seismometer clusters: Slip on the deep extension of the fault?, *Geophys. Res. Lett.*, **36**, L01303, doi:10.1029/2008GL036367.
- Sibson, R. H. (1984), Roughness at the base of the seismogenic zone: Contributing factors, *J. Geophys. Res.*, **89**, 5791–5799, doi:10.1029/JB089iB07p05791.
- Sun, S.-S., and W. F. McDonough (1989), Chemical and isotopic systematic of oceanic basalts: Implications for mantle compositions and processes, in *Magmatism in the Ocean Basins*, edited by A. Saunders and M. Norry, *Spec. Publ. Geol. Soc.*, **42**, 313–345.
- Thomas, A., R. Nadeau, and R. Bürgmann (2009), Tremor-tide correlations and near-lithostatic pore pressure on the deep San Andreas Fault, *Nature*, **462**, 1048–1051, doi:10.1038/nature08654.

- Trehu, A. M., and W. H. Wheeler (1987), Possible evidence for subducted sedimentary materials beneath central California, *Geology*, *15*, 254–258, doi:10.1130/0091-7613(1987)15<254:PEFSSM>2.0.CO;2.
- Wakabayashi, J. (1999), Subduction and the rock record: Concepts developed in the Franciscan Complex, California, in *Classic Concepts in Cordilleran Geology: A View From California*, edited by E. M. Moore, D. Sloan, and D. L. Stout, *Geol. Soc. Am. Spec. Pap.*, *338*, 123–135.
- White, R. W., R. Powell, and T. J. B. Holland (2007), Progress relating to calculation of partial melting equilibria for metapelites, *J. Metamorph. Geol.*, *25*, 811–827, doi:10.1111/j.1525-1314.2007.00711.x.
- Wintsch, R. P., R. Christofferson, and A. K. Kronenberg (1995), Fluid-rock reaction weakening of fault zones, *J. Geophys. Res.*, *100*, 13,021–13,032, doi:10.1029/94JB02622.

J. F. A. Diener and A. Fagereng, Department of Geological Sciences, University of Cape Town, Private Bag X3, Rondebosch 7701, South Africa. (ake.fagereng@uct.ac.za)